International Journal of Scientific and Technological Research
ISSN 2422-8702 (Online)
Vol 5, No.1, 2019

Comparison of jet transverse momentum resolution in large pile-up background at $\sqrt{s} = 7$ TeV

Nasuf Sonmez
Ege University, Faculty of Science, Physics Department, Izmir 35040, Turkey
E-mail: nasuf.sonmez@ege.edu.tr

Abstract
In this study, we focused on the jet transverse momentum resolution of the CMS detector, and the impact of high pile-up interactions on the jet p_T resolution is studied considering different jet finding algorithms. The jets are formed using the Anti-k_T and the Cambridge/Aachen jet finding algorithms with R=0.5, and the jet p_T resolution is investigated as a function of the average pile-up interactions that might take place in each collision. The properties of jets provide insight into the determination of many important observables in the colliders, and most importantly they allow to test the predictions of perturbative QCD and the new physics signals.

Keywords: Jet p_T resolution, Mc-Truth algorithm, Asymmetry method, Proton-proton collisions

1. Introduction

One of the powerful machines for making discoveries and testing the Standard Model (SM) [1] is the Large Hadron Collider (LHC) where proton-proton collisions are studied. There are two general purpose detectors at CERN. They are the ATLAS and the CMS experiments where protons are collided head-on at the center of the detectors. These two detectors are aimed to investigate the interactions among the constituents of the protons at the new energy regime. Protons are composite particles, and they consist of quarks and gluons. Historically, these gluons and quarks are called partons. Due to the confinement of the strong nuclear force, quarks and gluons, which are scattered off from the proton-proton collisions (pp), cannot be detected as free particles, but they reveal themselves as a stream of high energetic particles in the collision. These streams of high energy particles deposit some of their energies in electromagnetic and hadronic calorimeters, and by employing an algorithm which cluster all the energy related with each distinct parton in the collision the object called *jets* are formed. In a pp collider, jets are inescapable constituents, so they reveal themselves in each collision. They are also crucial for the discovery of new interactions and particles. After the very successful operation of the LHC in the last years, it entered high luminosity phase [2] where the number of protons in each collision, the collision frequency, and the center-of-mass energy are increased substantially.

At the LHC, protons are packed up as bunches (roughly 10^{11} protons), and they are smashed into each other at very high energies. In a high-luminosity mode, there is a non-negligible probability that one single bunch crossing may produce several head-on collisions, these will be separate events named as pile-up events. Every time these bunches cross each other, multiple collisions could take place. These collisions could contaminate the event which has something interesting in physics point of view. Detectors naturally observe all the particles produced in each bunch crossing, and the decay products coming from the collisions pile up on each other. Later, we track them back to determine which collision produced which particle. These pile-up events could be of the minimum-bias type, with diffractive and elastic events included. They could also be single and double diffractive events. In such an environment, the effect of multiple pp interactions need to be studied systematically so that their impact on a measurement could be understood and controlled.

Even though the CMS is powerful enough to measure the tracks and the energies of various particles created in each pp collision, determining the properties of all the particles produced in each collision with absolute precision is not possible. The energies of the jets, the energy scale of the hard scattering, and the jet p_T resolution are affected by the pile-up interactions. Since the discovery of a new particle is yielded by the observation of resonance, which looks like a peak at the spectrum, the pile-up interactions affect the width of these peaks. For better assessment of the detector output, the energy resolution needs to be determined correctly to handle the bumps and peaks which appear in the spectrum because they could be misidentified as a discovery of new particles related with the new physics. The number of

particles created in each collision changes naturally, and as a general-purpose detector, all of them need to be captured as efficient as possible. The CMS measures all these particles with a finite energy resolution. Besides, that energy resolution changes with the energy of the jets and the rapidity. The jets are formed by the clustering algorithm, and its energy is assigned merely by summing all the energy deposited in the calorimeters.

There are various methods used in the CMS to determine the energy resolution of jets as a function of the rapidity and the energy (or the transverse momentum of the jets, p_T). One of the methods is merely simulating various jets coming from the scattered partons, and these reconstructed jets are paired with generation level jets. After sorting these jets according to their transverse momentum and rapidity, the response in each of the energy range is calculated, and the resolution as a function of the energy could be obtained. This method is called the *MC-Truth*. It could only be used for the Monte Carlo simulated jets because it is not possible to match the partons with the jets in real life. Another method is called the *Asymmetry* method. The asymmetry is calculated for back-to-back jets, and their average energy shift is determined for predefined energy intervals. This method is used in a previous collider Tevatron [3], it is still in use at the CMS detector. In this study, we focused on the jet p_T resolution, and the results are presented employing these two algorithms (Mc-Truth and Asymmetry) considering the CMS detector. The impact of a large pile-up on the jet p_T resolution is investigated for different jet finding algorithms; They are Anti-k_T and Cambridge/Aachen jet finding algorithms with $R = 0.5$.

The content of this paper is organized as follows. In section 2, Monte Carlo simulation of the pp collisions and the data samples used in the analysis are given. In section 3, the response of the reconstructed jets is calculated, then jet p_T resolution is calculated using MC-Truth algorithm. The Asymmetry method is explained, and an example is given in section 4. Further, the energy resolution in a high pile-up environment is studied, and the results are given in section 5. The conclusion is drawn in sec 6.

2. Monte Carlo simulation and data sample

The parton level collision events at the CMS detector are generated using PYTHIA-6 [4] and MADGRAPH [5], and the full simulation of these events is accomplished with DELPHES[6]. Full simulation means dressing the events with parton-shower and hadronization, then reconstructing the jets with various jet finding algorithms. In Figure 1, a pictorial representation of a proton-proton collision is drawn. The possible hard interaction between the partons is represented by *big red blob*. The decays of the final state particles are represented by *small red blobs*. The hard QCD radiation is indicated by the *red wiggly lines*. The secondary kind of interaction between the rest of the protons takes place (*purple blob*), and it is called the underlying event. Before going into hadronization stage, the partons are represented by *light green blobs*, and the decay of the hadrons are given with *dark green blobs*. Finally, the photon radiation, which could happen at any stage, is pictured by *yellow* lines.

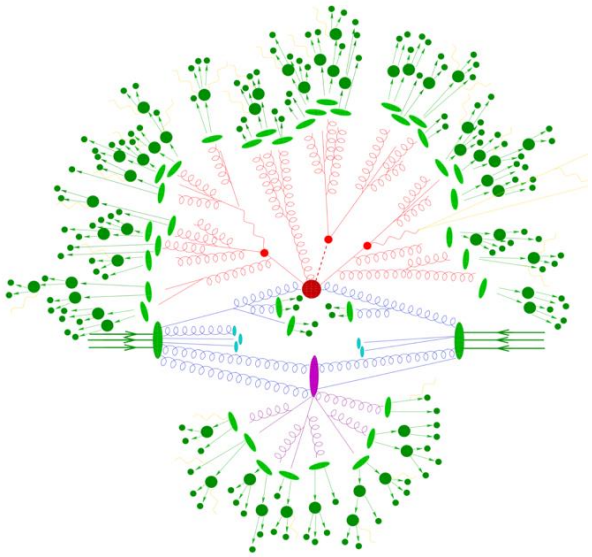

Figure 1. Pictorial representation of a collision event which is produced with Monte Carlo event generator. The graphic is taken from Ref. [7].

A sample of QCD Monte Carlo events are produced using PYTHIA-6 with flat-p_T (total transverse momentum of jets) using bins given in Table 1 at $\sqrt{s} = 7$ TeV. This data sample consists of 10 million pp collision events. The jets are reconstructed using Anti-k_T jet finding algorithms with $R = 0.7$. This sample is merely produced to explain the MC-Truth and the Asymmetry methods, and how the jet p_T resolution is extracted from the data. Since the CMS detector has a finite resolution, jet spectrum and all other related physical distributions such as energy, momentum, and rapidity need to be plotted in a finite width bin. For example, if one needs to draw a histogram with the p_T as a free parameter, the width of the bins needs to be proportional with the computed p_T resolution. Besides, the value of the resolution needs to be roughly close to the value at the center of each bin.

Table 1. Jets are binned with the following p_T ranges.

53	67	81	97	114	133	153	174	196
220	245	272	300	330	362	395	430	468
507	548	592	638	686	737	790	846	905
967	1032	1101	1172	1248	1327	1410	1497	1588
1684	1784	1890	2000	2116	2238	2366	2500	2640

For the pile-up study the events are generated with MADGRAPH [5]. Events are dressed with parton-shower and hadronization using PYTHIA-6, then the reconstruction of jets and their kinematical variables are calculated using DELPHES. The following HT-bin intervals are assumed in pure QCD events (100-250, 250-500, 500-1000, 1000-2000, 2000-3000, and 3000-Infinity) with the following *xqcut* variables $(30, 30, 40, 40, 40, 40)$ GeV, respectively. The scattering process is assumed as $pp \rightarrow 2, 3,$ and 4 jets with minimum jet transverse momentum of $p_T = 20$ GeV. In the study, only jets in the central region ($\eta < 2.4$) are used. Roughly more than 1 Million events are produced for each HT-bin. HT is defined as scalar sum of the transverse momentum of all jets produced in each event. Jets are matched by MLM [8] matching algorithm. The same events are reconstructed with the inclusion of varying the number of pile-up collisions in each event. The pile-up events include the minimum-bias type with diffractive and elastic events. The response of the detector is computed with the pile-up values (0, 10, 25, 50, 100, 150). Next, Anti-k_T and Cambridge/Aachen jet finding algorithms are used for clustering the deposited energy in calorimeter towers. The matching criteria for the reconstructed jets is based on the angular distance, and $\Delta R < 0.25$ is used to associate particle-level jets and detector-level jets.

3. Jet transverse momentum resolution using method 1

Jet transverse momentum resolution is simply the quantified momentum/energy spread of the reconstructed jets. First, events with pure QCD collisions are generated, and jets are formed by the jet finding algorithms after employing the parton shower and the hadronization on the scattered quarks and the gluons. These jets are called the *generated jets* (*GenJet*) because they include every possible information coming from the generation step, even the intrinsic quantum numbers which cannot be known in the real world. Then, the instrumental effects need to be included on all the partons in each collision, thus the parton-shower, the hadronization step, and the detector response are fully simulated for these particles using PYTHIA+DELPHES. In this step, the energy deposited in the calorimeter towers for all the particles in the collision are obtained. Next, these calorimeter towers are clustered together using the same jet finding algorithms which are used in the formation of GenJets, these objects are called *reconstructed jets* (*RecoJet*). As a result, we construct two objects for each parton, they represent two distinct realities in different views. Since these two objects correspond to the same scattered partons, the GenJets could be considered as the reference objects of the RecoJets. The reconstructed jets include all the instrumentation and algorithm related deficiencies just like in real life. After the simulation step, all the reconstructed jets in each event are matched with the generated jets. The matching is performed merely on two-dimensional $\eta - \phi$ space of the detector, GenJets and RecoJets are paired, if they are close to each other within $\Delta R = \sqrt{(\Delta\phi)^2 + (\Delta\eta)^2} < 0.2$ cone. Besides, if there are multiple jets in the same cone, then the closest ones are matched to each other. This algorithm is called the MC-Truth

matching algorithm, and all reconstructed jets are paired with a generated level jets to calculate the response and the jet p_T resolution.

Response

After employing the MC-truth algorithm, the simulated jets are matched with GenJets. The energy of the GenJets could be considered as the initial energy of the parton, thus it could be considered as the true energy of the jet. Therefore, the ratio of the detector-level (reconstructed) transverse momentum of the jet (p_T^{reco}) to particle-level transverse momentum of the jet (p_T^{gen}) is simply called the response.

$$\text{Response} = \frac{p_T^{\text{reco}}}{p_T^{\text{gen}}} \tag{1}$$

Next, the MC-Truth method is employed for all jets in each event, and the ratios ($p_T^{\text{reco}}/p_T^{\text{gen}}$) are calculated for the jets with the highest p_T in each event. Then, the ratios are filled into histograms for each p_T interval defined in Table 1. The response of the highest p_T jets are drawn in Figure 2 for random four bins with $0 < |y| \leq 0.5$ rapidity region; the jets are formed using Anti-k_T jet finding algorithm with $R = 0.7$. In Figure 2, it can be seen that the central region resembles a Gaussian distribution, and the tail on each side is exponentially dropped. Besides, at high p_T ranges the peaks become narrower. That means the detector has a greater resolution at high p_T ranges. In other words, the detector measures the jets p_T with high precision at high p_T values than the low p_T jets.

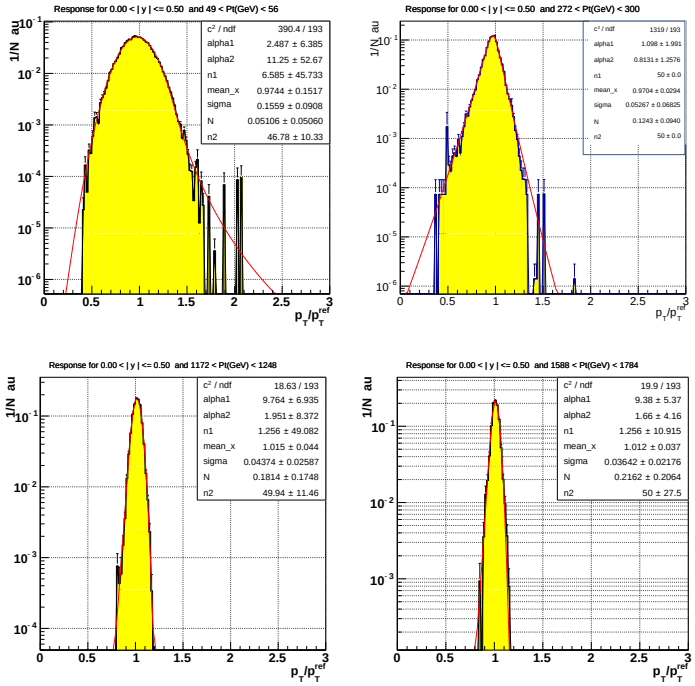

Figure 2. Jet p_T responses in four different p_T ranges are given for central (0<|y|<0.5) rapidity region. The central region in each peak is fitted using the Gaussian peak, and the exponential decay at both of the tails are fitted using the Crystal-Ball function. The figures are obtained with *flatQCD* data sample, Anti-k_T jet finding algorithm with R=0.7.

Next, we need to determine the mean value of these peaks, and also the standard deviation to calculate the resolution. In Figure 2, we could use the Gaussian distribution naturally for the central region, but the tails on both sides need a different approach. Away from the central region, sharp exponential decay is seen in all the response distributions, the *Crystal-Ball* function [9] fits for these regions. Accordingly, a function which consists of a Gaussian peak at the central region and Crystal-Ball function for each side of the tails, which represents the exponential decay, is constructed, and it is defined as follows:

$$f(x;\alpha_i,n_i,\overline{x},\sigma) = N \cdot \begin{cases} A_1(B_1 - \frac{x-\overline{x}}{\sigma})^{-n_1}, & \alpha_1 \leq \frac{\overline{x}-x}{\sigma} \\ \exp(\frac{-(x-\overline{x})^2}{2\sigma^2}), & \alpha_1 < \frac{\overline{x}-x}{\sigma} \leq \alpha_2 \\ A_2(B_2 - \frac{x-\overline{x}}{\sigma})^{-n_2}, & \frac{\overline{x}-x}{\sigma} \leq \alpha_2 \end{cases} \quad (2)$$

where $A_i = \left(\frac{n_i}{|\alpha_i|}\right)^{n_i} \cdot e^{-\frac{|\alpha_i|^2}{2}}$, $B_i = \frac{n_i}{|\alpha_i|} - |\alpha_i|$, N is the normalization factor, and $\overline{x}$ and σ represent mean value and standard deviation of the Gaussian peak at the central region, respectively. Finally, α_i and n_i represent the exponential decay of the tail region on the left and on the right hand side of the peak. Next, with the help of MINUIT [10,11] package, the fit is employed on each response distribution, and the standard deviation (σ) and the mean value ($\langle p_T/p_T^{ref} \rangle$) are obtained. In Figure 2, the fitted function is plotted in four p_T ranges with $0 < |y| \leq 0.5$ where the red-line represents the fitted function with equation 2. The same calculation is continued for the rest of the rapidity regions, and the same ratio is obtained up to $|\eta| < 2.5$.

Jet transverse momentum resolution

After fitting with the Gaussian and the Crystal-ball functions, the mean value $\langle p_T/p_T^{ref} \rangle$ and the standard deviation ($\sigma(p_T)$) obtained for each p_T-bin. The energy resolution is defined as the ratio of these computed values ($\frac{\sigma(p_T)}{p_T}$). Then, energy resolution is computed for each p_T-bin using these values, and the ratios are plotted for the corresponding p_T values in Figure 3 where the resolution distribution is given for the two rapidity regions. The energy resolution is expressed with the following equation [12,13].

$$\text{Resolution} = \frac{\sigma(p_T)}{p_T} = \sqrt{\left(\frac{A}{p_T}\right)^2 + \left(\frac{B^2}{p_T}\right) + C^2} \quad (3)$$

where p_T is the transverse momentum of the jets, $\sigma(p_T)$ is the standard deviation of the Gaussian function fitted to the calorimeter response distributions. The meaning of the terms A, B, and C [14] used in the definition of the momentum resolution of jets at CMS are given as follows:

- *Stochastic Noise Term (A)*: This term represents the noise caused by to fixed energy fluctuations in the cone from electronic noise, pile-up and underlying event activity.
- *Electronic Noise (B)*: This term is related with the electronic noise of the measurement of the analog signa, it is effective at low energies. It comes from the stochastic response of the calorimeter measurements. It is modeled with *Poisson* statistics.
- *Constant Term (C)*: This term represents residual non-uniformity and non-linearity in the detector response. It is constant with no p_T dependency.

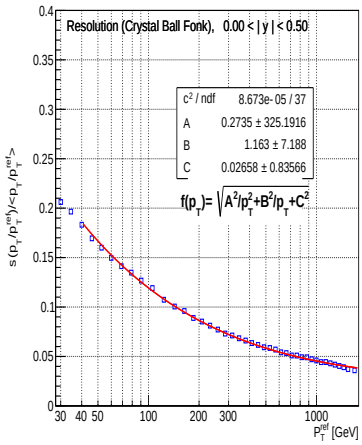

Figure 3. Jet p_T resolution as a function of p_T in $0 < |y| \leq 0.5$ rapidity region. Black circles are obtained using MC (*flatQCD*) simulation with Anti-k_T, no pile-up, and $R = 0.7$. The red line represents the fitting function using Eq. 3.

In Figure 3, the jet p_T resolution is fitted with Eq. 3, and the factors A, B and C are also depicted there. It should be noted that MC-Truth method could not be used at the detector level objects, and its usage is merely for setting the lowest possible jet transverse momentum distribution, that is any other method, that uses the detector level objects, should not obtain lower values.

4. Jet transverse momentum resolution using method 2

In this method, jets are sorted according to their transverse momentum, and the highest two of them are checked whether they are back-to-back in azimuth angle (ϕ). Then, the asymmetry (A) is defined for each event, and the response is calculated with a formula which will be defined later. The jet p_T resolution is computed using the same function defined in Eq. 3. The calculation is employed using the same events with the previous example. Since there are 10 million events, they are enough to demonstrate the method. The asymmetry is defined as follows:

$$\text{Asymmetry} = \frac{p_T^{jet1} - p_T^{jet2}}{p_T^{jet1} + p_T^{jet2}}, \tag{4}$$

where p_T^{jet1} and p_T^{jet2} are defined as the jets with the highest transverse momentum and the second highest one, respectively. This method needs to be employed using the jets that are happened to be back-to-back. The events could easily be filtered out by applying the following cut $(\phi_{jet1} - \phi_{jet2})/\pi > 0.9$. However, this is not the situation, in reality, it is possible that the events are really in di-jet topology, and due to the instrumentation and the reconstructing algorithms jets could be constructed not resembling the hard scattering. Therefore, to account all these effects, various constraints are applied to the third highest jet in each event. The constraints are given as follows: $p_T^{3-jet} < 8, 15, 20, \text{and } 30$ GeV, the asymmetry is calculated for each case. In Figure 4, the asymmetry is plotted for the same p_T intervals defined in Table 1. It can be seen in the Figure 4 that the asymmetry distribution is centered roughly around 0 in all the p_T-bins. The same observations with the previous method are seen that the distribution gets narrow at high p_T-bins. In Figure 4, the asymmetry distribution for four p_T interval depicted in each of the figures are given assuming the third highest jet's transverse momentum is less than 8 GeV ($p_T^{3-\text{jet}} < 8$ GeV).

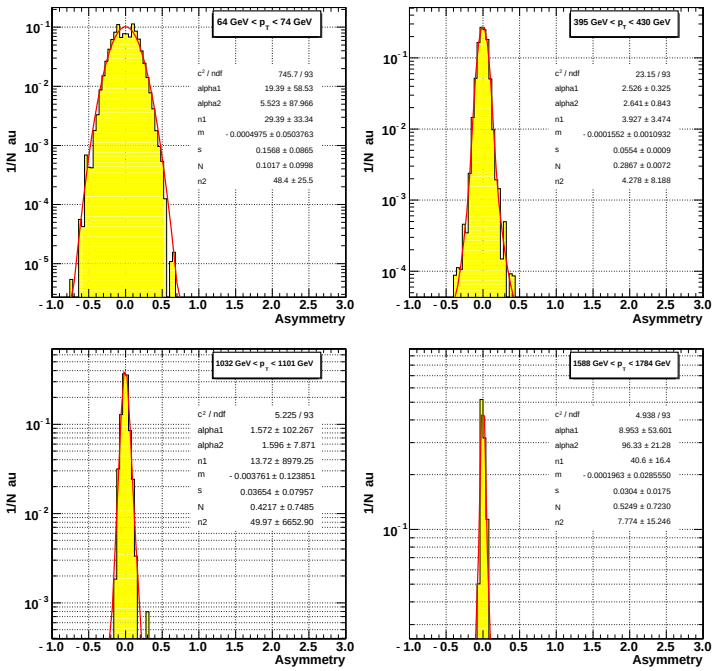

Figure 4. The asymmetry distributions in four distinct p_T bins, and a fitting function consists of the Gaussian and the Crystal-Ball is used in each p_T interval. The figures are obtained using *flatQCD* data sample, Anti-k_T jet finding algorithm with $R = 0.7$, $|y| < 2.5$, and $p_T^{3-jet} < 8$ GeV constraint.

The same method is followed, using Eq. 2 each of the distribution is fitted, and the relevant parameter σ_A for the fit is obtained. The relation between the standard deviation of the Gaussian peak σ_A and the jet p_T resolution is defined as follows:

$$\left(\frac{\sigma(p_T)}{p_T}\right) = \sqrt{2}\sigma_A \quad (5)$$

The jet p_T response is computed accordingly for all the p_T-bins. Next, the same calculation is carried out for the rest of the constraints ($p_T^{3-jet} < 15$, 20, and 30 GeV). The jet p_T resolution as a function of the p_T^{3-jet} is plotted in Figure 5 for two intervals. Next, a linear fit is applied, and using the linear extrapolation the jet p_T resolution at $p_T^{3-jet} \approx 0$ GeV is calculated for all the p_T intervals.

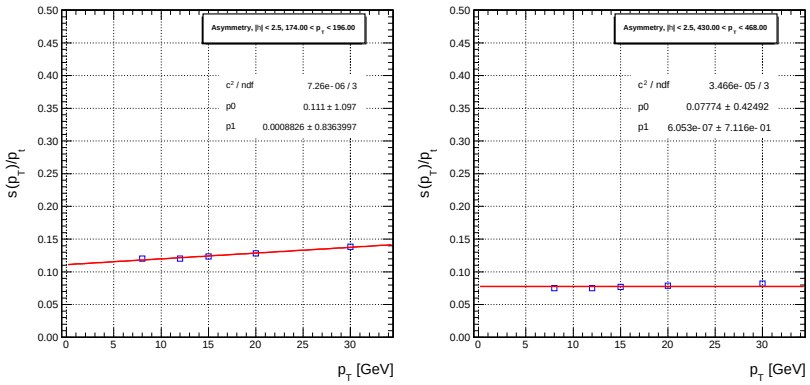

Figure 5. Jet $p_T$resolution on two different p_T-bins depicted in each figure as a function of the third highest jet's transverse momentum. Linear extrapolation is employed, and the resolution is calculated at $p_T^{3-jet} \approx 0$ GeV. *flatQCD* data, Anti-k_T jet finding algorithm with $R = 0.7$ and $|y| < 2.5$.

Finally, the jet p_T resolution distribution is obtained for all the p_T-bins. In Figure 6, the distribution of the jet p_T resolution is given for $p_T^{jet3} < 30$ GeV (left), $p_T^{jet3} < 8$ GeV (right), and the extrapolated one $p_T^{jet3} \approx 0$ GeV (bottom). The next step is to parameterize the distribution of the final jet p_T resolution with the same Eq. 3. The parameters A, B and C are obtained after fitting each of the distribution with MINUIT, and they are depicted in Figure 6.

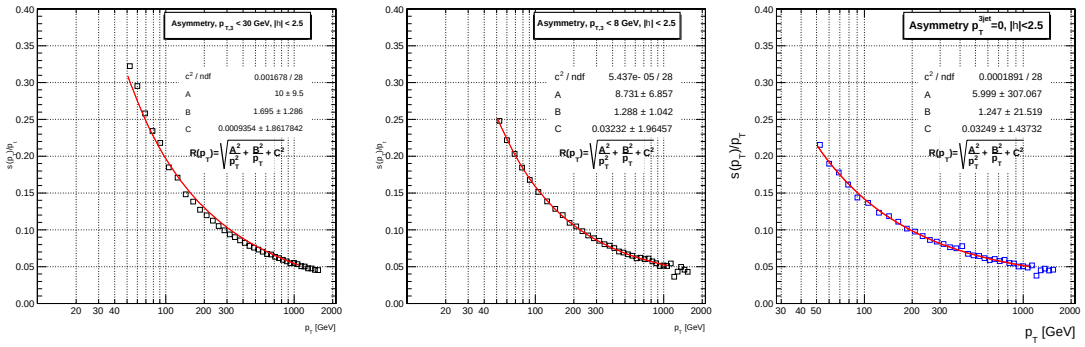

Figure 6. Jet p_T resolution using the Asymmetry method with various p_T^{3-jet} cuts on the third jets transverse momentum in $|y| < 2.5$ region, *flatQCD* data, Anti-k_T algorithm with $R = 0.7$. (left): jet p_T resolution with constraint $p_T^{3-jet} = 30$ GeV, (center): jet p_T resolution with constraint $p_T^{3-jet} = 8$ GeV. (right): jet p_T resolution with the extrapolation $p_T^{3-jet} \approx 0$ GeV.

5. Jet transverse momentum resolution in high pile-up environment

Extracting the transverse momentum resolution of the jets is vital for discovering new particles and particularly the estimation of systematical errors in the results, and also for not missing the prominent discoveries [15,16]. In this study, pile-up interactions are taken into consideration in pp collisions, the average numbers of collisions per bunch-crossing, $\overline{n}$, are set as following: 0, 10, 25, 50, 100, and 150 using the MADGRAPH simulated data. The jets are reconstructed using Anti-k_T and Cambridge/Aachen algorithms with $R = 0.5$ cone size. These pile-up events are assumed as the minimum-bias type with events of diffractive (single and double diffractive) and elastic physics. The methods described for the

MC-Truth and the Asymmetry are employed for the data sets calculated with the various number of average pile-up interactions in each bunch-crossing.

MC-Truth method

The events are binned according to the highest jet's p_T, the response is calculated by matching these jets with the generation level jets. The jet p_T spectrum is binned with Table 1. Then, each response distribution is fitted with the function defined in Eq. 2 (Gaussian peak at the central values with Crystal-ball functions at the tails), and the mean and the standard deviation is extracted for every p_T bin. Next, the resolution is calculated for each of the bin, and they are plotted as a function of the corresponding p_T^{gen} in Figure 7 for Anti-k_T (left) and Cambridge/Aachen (right) algorithms, respectively.

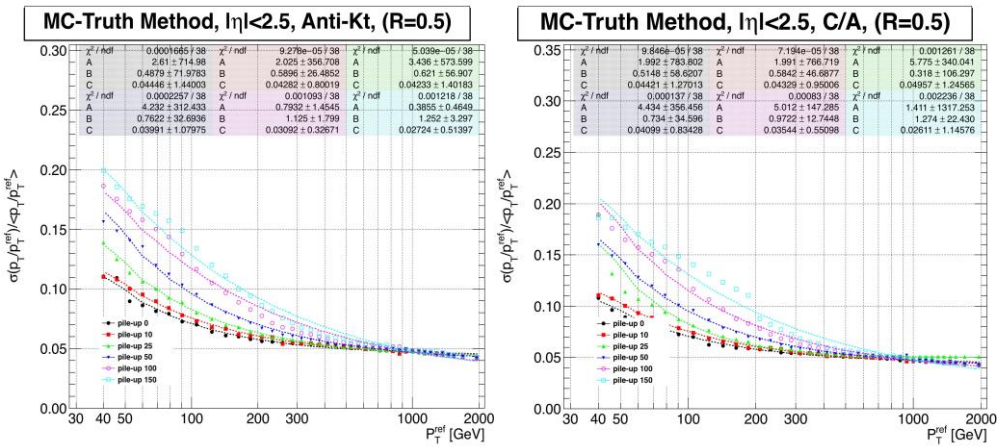

Figure 7. The jet p_T distributions as a function of the average pile-up interactions using the MC-truth algorithms. The distributions are plotted with Anti-k_T (left) and Cambridge/Aachen (right) jet finding algorithm. MADGRAPH event generator, with R=0.5 cone size.

The calculation is carried out for the other simulated samples with varying pile-up numbers, the distributions are also given in Figure 7. Finally, each distribution is fitted with Eq. 3, and the jet p_T resolution is quantified as a function of the average pile-up numbers. Comparing the jet p_T distributions of the Anti-k_T and the Cambridge/Aachen algorithms concludes that the difference between them is almost negligible. It can be seen that the distribution of jet p_T resolution gets higher in increasing pile-up in both of the figures, this is expected since the number of pile-up interactions pollutes the event, and particularly energy deposited in each of calorimeter cell increases. The resolution is at $p_T = 50$ GeV is in $0.1 - 0.18$ range for average $0 - 150$ pile-up numbers. At higher p_T values the jet resolution gets lower in all pile-up scenarios and both of the jet finding algorithms. Over all the jet p_T resolution reaches to ~ 0.45 for $p_T > 1000$ GeV.

Asymmetry method

The p_T response is calculated in similar ways described for the Asymmetry method. Two of the jets with the highest transverse momentum are selected, and the asymmetry is computed, histograms with the asymmetry distributions are filled for each of the p_T-bins given in Table 1. The center of each asymmetry distribution is fitted with the Gaussian peak at the central with Crystal-ball functions at the tails, and only the standard deviation is calculated for every p_T bin interval. Next, the resolution distribution is obtained for Anti-k_T and Cambridge/Aachen jet finding algorithms, and also the different pile-up scenarios. The distributions of the jet p_T resolution are plotted as a function of p_T^{mean} in Figure 8.

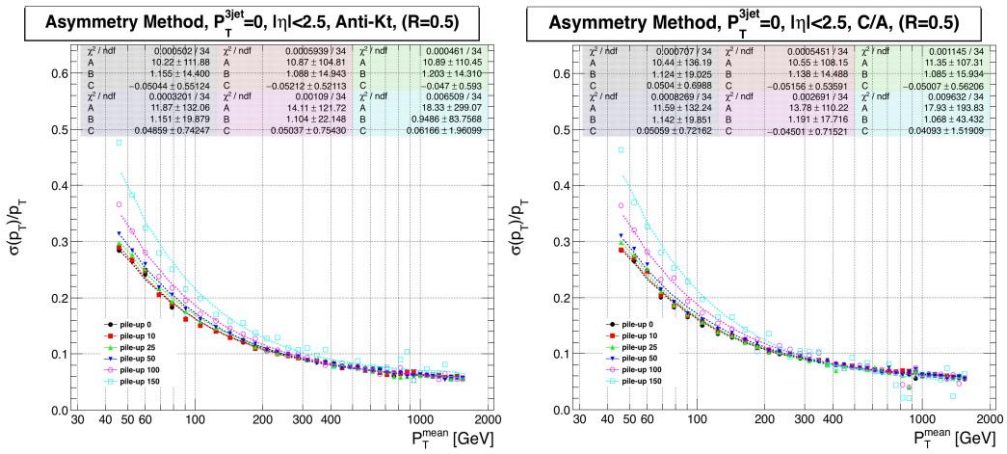

Figure 8. The jet p_T distributions as a function of the average pile-up interactions using the Asymmetry. The jet p_T resolutions are plotted with Anti-k_T (left) and Cambridge/Aachen (right) jet algorithm. MADGRAPH event generator, with R=0.5 cones size.

The distributions are fitted with Eq. 3, and the jet p_T resolution is obtained as a function of the average pile-up numbers. The fitting factors A, B, and C are also depicted in each of the figures.

6. Summary and Conclusion

In this study, various methods used in determining the jet p_T resolution are presented; they are namely the MC-Truth and Asymmetry methods. These methods are useful to determine the jet transverse momentum resolution, and comparing Figure 3 and 6 (right) shows that jet transverse momentum is spread at low p_T values, and it drops at increasing p_T regions. Both methods show that the detector could measure the jet p_T at higher precision in higher energies. However, applying the MC-Truth method reveals that the obtained resolution $(\sigma(p_T)/p_T)$ is lower than the Asymmetry method, in a way it exhibits better precision. The reason is that the MC-Truth method uses the parton level information, and thus the match is better. However, the MC-Truth algorithm cannot be used in real life, and therefore it serves to set or determine the minimum jet resolution that any detector could have. Thus, the jet p_T resolution which is obtained by the Asymmetry or any other method could not have lesser values. The p_T resolution gives us a measure of uncertainty related to the jet p_T measurements.

These methods are applied to compute the transverse momentum resolution with various pile-up scenarios and jet finding algorithms considering the CMS detector at $\sqrt{s} = 7$ TeV. The distributions of jet p_T resolution are calculated with increasing pile-up for both the Anti-k_T and the Cambridge/Aachen jet finding algorithms. The results show that the uncertainty in the estimation of the jet p_T resolution decreases in higher p_T ranges. Also, the smearing effects are crucial, and their effects are dramatic at low energies; therefore, the uncertainty gets higher which means the p_T resolution worsens. Determining the jet p_T resolution is essential for obtaining better precision in hadron colliders. For example, estimating the jet p_T resolution is critical to get the jet energy spectrum correctly which is used to recover the inclusive jet cross section. Therefore, resolving the pile-up effects, the instrumental, and other non-linear issues make it possible to unfold their impact from the real collision data. Besides, having a better jet p_T resolution effects the discovery potential of the new physics related signals which reveal themselves with soft jets in the detector.

Acknowledgements

The numerical results reported in this paper were partially performed at CERN and FERMILAB. This work is supported by TAEK project No: CERN-A5.H2.P1.01-16. Part of the calculation is done at TUBITAK ULAKBIM, High Performance and Grid Computing Center (TRUBA resources).

7. References

[1] W. N. Cottingham and D. A. Greenwood, An introduction to the standard model of particle physics (Cambridge University

Press, 2007).
[2] O. Brüning and L. Rossi, Adv. Ser. Direct. High Energy Phys. 24, pp.1 (2015).
[3] B. Abbott et al. (D0), Nucl. Instrum. Meth. A424, 352 (1999), arXiv:hep-ex/9805009 [hep-ex].
[4] T. Sjostrand, S. Mrenna, and P. Z. Skands, JHEP 05, 026 (2006), arXiv:hep-ph/0603175 [hep-ph].
[5] J. Alwall, M. Herquet, F. Maltoni, O. Mattelaer, and T. Stelzer, JHEP 06, 128 (2011), arXiv:1106.0522 [hep- ph].
[6] J. de Favereau, C. Delaere, P. Demin, A. Giammanco, V. Lemaître, A. Mertens, and M. Selvaggi (DELPHES 3), JHEP 02, 057 (2014), arXiv:1307.6346 [hep-ex].
[7] A. Schaelicke, T. Gleisberg, S. Hoeche, S. Schumann, J. Winter, F. Krauss, and G. Soff, Heavy ion reac- tion from nuclear to quark matter. Proceedings, International School of Nuclear Physics, 25th Course, Erice, Italy, September 16-24, 2003, Prog. Part. Nucl. Phys. 53, 329 (2004), arXiv:hep-ph/0311270 [hep-ph].
[8] J. Alwall et al., Eur. Phys. J. C53, 473 (2008), arXiv:0706.2569 [hep-ph].
[9] J. E. Gaiser, Charmonium Spectroscopy From Radiative Decays of the J/ψ and ψ, Ph.D. thesis, SLAC (1982).
[10] F. James and M. Roos, Comput. Phys. Commun. 10, 343 (1975).
[11] A. Lazzaro and L. Moneta, Proceedings, 17th International Conference on Computing in High Energy and Nuclear Physics (CHEP 2009): Prague, Czech Republic, March 21-27, 2009, J. Phys. Conf. Ser. 219, 042044 (2010).
[12] O. Kodolova, Phys. Part. Nucl. Lett. 5, 13 (2008).
[13] S. Chatrchyan et al. (CMS), JINST 6, P11002 (2011), arXiv:1107.4277 [physics.ins-det].
[14] C. W. Fabjan and F. Gianotti, Rev. Mod. Phys. 75, 1243 (2003).
[15] F. Nebeker, Historical Studies in the Physical and Bio-logical Sciences 25, 137 (1994).
[16] Luc Demortier, “Real, false and missed discoveries in high energy physics,” url: http://physics. rockefeller.edu/luc/talks/HEPDiscoveries.pdf (2008).